

Nonlinear Switching Dynamics in Surface Electromyography of the Spine

P. Lohsoonthorn and E. Jonckheere
Department of Electrical Engineering–Systems
University of Southern California
Los Angeles, CA 90089-2563
jonckhee@eudoxus.usc.edu, <http://eudoxus.usc.edu>

Abstract

This paper develops a switching dynamics model of the surface Electromyographic (sEMG) signal generated during a condition in which the mechanical attachment of the spinal dura to the cervical vertebra creates an unstable nonlinear feedback coupling between the biomechanics of the spine and the central nervous system (CNS). The sEMG signal recorded on the paraspinal muscles during this condition reveals “bursts” of accrued sEMG activity interrupting an otherwise quiet “background” signal. Statistical analysis of the autocorrelation and partial correlation functions of the burst and background parts of the signal reveals that the overall signal indeed switches between two modes. Both the burst and the background modes are dynamically modeled by ARIMA and ACE, and a switching logic, driven by the autocorrelation and the partial correlation, is designed, resulting in a switching model that matches the experimental sEMG signal fairly well.

1 Introduction

In a book [2] that has captured the attention of spine health professionals, the Scandinavian neurosurgeon Alf Breig introduced the concept of *Adverse Mechanical Tensions in the Central Nervous System*. The tenet of this theory is the fact that the dura mater of the spinal cord is mechanically attached to the gutter of the transverse process at the 4th to 6th cervical segments, so that, say, vertebral misalignment or postural problems can create pathological tensions on the spinal cord, themselves impairing nerve activity. Tensions in the spinal cord induce hyperstimulation of the proprioceptive fibers afferent to the spine, resulting in impaired functionality of the spine at the attachment level and other effects at other parts of the nervous system. It has been argued by Breig that some diseases have this neuro-biomechanical origin and that relieve of these adverse tensions could alleviate symptoms [3].

More closely related to the present paper is the fact that dural attachments appear to create extra feedback paths from the mechanical movement of the spine to the CNS. In the motor

reflex loop, the degree of stretch of the paraspinal muscles is recorded by the neuromuscular spindles and transmitted by afferent fibers to the motor neurons in the spine, back to the muscles via the efferent fibers [10, p. 41, 139]. However, the dural attachment creates an extra feedback path from the paraspinal muscles *directly* to the spinal neurons. The existence of this extra feedback path has been demonstrated by a technique referred to as *Network Spinal Analysis (NSA)*. In this technique, the practitioner locates the spinal gateway, which is on the skin overlying or in the vicinity of the dural-vertebral attachments, based on his (her) professional assessment of the status of the active, passive, and neural subsystems supporting the normal function of the nervous system [9], and sensitizes the areas to the point where a slight pressure at the spinal gateway elicits an oscillation that takes the form of a spontaneous, involuntarily controlled rocking motion of the spine. This produces a rather intensive exercise for the spine and the back musculature, not reproducible by any other physiotherapeutical means. This kind of involuntary physical activity has shown therapeutic benefits for a five years post injury quadriplegic patient [8].

A long term objective of this project is to achieve a better understanding of the dural attachment and the nonlinear feedback mechanisms occurring there. The shorter term objective of the present paper is to analyze what is probably the most fundamental aspect of the sEMG signal—namely, that the sEMG signal consists of “bursts” of accrued sEMG activity interrupting a quiet, background signal.

An outline of the paper follows: In Section 2, the intuitive burst versus background discrimination is given a rigorous, objective interpretation in terms of the so-called autocorrelation and partial correlation functions. The (incremental) burst signal is distinguished from the (incremental) background signal as being more stationary as revealed by a faster decaying autocorrelation. After this statistical discrimination analysis, in Section 3, the Box-Jenkins procedure for building linear stationary models for time series [5] is used to obtain models for these two different signals. In Section 4, as a follow up on ARIMA modeling, we check heteroskedasticity, that is, time varying variance, of the residual error. In Section 5, the Alternating Conditional Expectation (ACE) [4] is used to evaluate nonlinear models

for each separate mode, with a significant improvement over linear models for the burst dynamics and not much improvement for the background dynamics. Finally, in Section 6, a switching logic between the two dynamical modes based on the mean square average of the autocorrelation and the partial correlation functions is developed. It is shown that the two linear models along with the switching logic provide a good model of the overall signal.

2 “Bursty” versus “Quiet” Signal Discrimination

Consider the full neck signal $\{y(t)\}$ of Figure 1 from an anonymous patient, recorded by means of noninvasive electrodes at a sampling frequency of 4,000 samples per second. This patient gave the investigators *Informed Consent to Participate in Research* under a protocol approved by the *Institutional Review Board* of the University of Southern California.

It is obvious that this signal switches between two different “modes.” To unravel the fundamental statistical properties of the signal, and confirm the visually intuitive feature that it transits between different modes, consider the plot of Figure 3, showing the sample autocorrelation and partial correlation functions of the full signal. The slow decay of the sample autocorrelation is a first indication of a lack of stationarity. Furthermore, the sample partial correlation function, shown in the same Figure 3, has value almost equal to one at lag one, which indicates the possible presence of a unit root. The later is confirmed by the Dickey and Fuller test indicating that the signal indeed has a unit root. All of these features indicate that a first order difference should be applied to this signal, viz.,

$$x(t) = y(t) - y(t-1)$$

This incremental signal is shown in Figure 2. Like the raw signal, this incremental signal shows areas of “bursts” and areas of quiet sEMG activity, probably in a more marked way than the raw signal.

The statistical analysis of this incremental signal dictates the breaking of the signal into two components: A “burst” part running from time point 1 to time point 5,000 and the complementary “background” part running from time point 5,000 to time point 7,500. The sample autocorrelation and sample partial correlation functions of the burst (background) signal have been computed and are shown in the plots of Figure 4 (5). On the one hand, the autocorrelation of the burst signal decreases very fast. On the other hand, the autocorrelation of the background signal decreases very slowly. *This discrepancy in the rate of decay of the correlation is used as the formal—and objective—discrimination between the burst signal and the background signal.* Quantitatively, we use the absolute summation of the sample autocorrelation function to discriminate the burst signal from the background signal; that is, the signal is a

burst (background) signal if the absolute summation of the sample autocorrelation is smaller (greater) than a certain threshold. For this particular signal, the absolute summation of the sample autocorrelation function runs from lag 1 to lag 20 and the threshold is set to 2.5. The absolute summation of sample autocorrelation and absolute summation of sample partial correlation functions have been computed from the subsignals $\{x(T+1), \dots, x(T+500)\}$ for $T = 0, 500, \dots, 159500$ and are plotted versus T in Figure 6.

A rather surprising fact is that the discrimination between the “burst” part and the “background” part of the signal does not quite coincide with the intuitive, naked eye analysis of the raw sEMG signal classifying as “bursty” an area of accrued sEMG activity. However, the same intuitive, naked eye analysis applied to the *incremental signal* yields results somewhat more consistent with the rigorous mathematical analysis.

3 Linear ARIMA Modeling

From the previous section, we know that the behaviors of the burst signal and the background signal are different. Hence we develop two separate models—one for the burst signal and one for the background signal. The signal $y(t)$ from time point 1 to time point 5,000 is considered as a prototype for the burst signal. The signal $y(t)$ from time point 5,000 to time point 7,500 is considered as a prototype for the background signal.

For the burst signal $y(t), 1 \leq t \leq 5,000$, the Smallest CANonical (SCAN) correlation method and the Extended Sample Autocorrelation Function (ESACF) method [1] are used to identify the orders of the stationary or nonstationary models of the burst signal as ARMA $(p+d, q)$. Because both the SCAN and ESACF methods indicate that $p+d \geq 1$, a unit root test should be used to determine whether this term of degree $p+d$ is a unit root or an autoregressive term. The augmented Dickey-Fuller Unit Root Test [5] indicates that this signal should be considered as a nonstationary signal with unit root. Similar procedure is applied to the first order difference signal $x(t) = (1-L)y(t)$, where L denotes the unit delay. However, the augmented Dickey-Fuller Unit Root Test [5] fails to indicate that this signal $x(t)$ should be considered as a nonstationary signal with unit root. Therefore, the models are of the ARIMA $(p, 1, q)$ type, meaning that the one-fold incremented signal $(1-L)y(t) = x(t)$ can be modeled as the output of a filter $\frac{N_q(L)}{D_p(L)}$, where N_q, D_p are polynomials of degree q, p , respectively, in L , driven by a white noise $\varepsilon(t)$. The tentative model transfer functions $\frac{N_q}{D_p}$ for the burst signal are as follows:

$$\begin{aligned} \text{ARIMA}(1, 1, 1) &: \frac{(1-0.7781L)}{(1-0.3509L)} \\ \text{ARIMA}(1, 1, 3) &: \frac{(1-1.363L+0.2258L^2+0.1374L^3)}{(1-0.9019L)} \end{aligned}$$

Table 1: Mean square error for the prediction of the burst signal from time point 1 to time point 5,000.

Model	Mean Square Error
ARIMA(1, 1, 1)	95, 539
ARIMA(1, 1, 3)	92, 156

From the tentative models for the burst signal, it turns out that the ARIMA(1, 1, 3) is the best model for $y(t)$ in the sense that it corresponds to the least mean square error. Table 1 shows the mean square errors for the one-step prediction of the models of the burst signal.

It is observed from Figure 7 that the one step prediction of the burst signal does not compare well with the actual burst signal. It can be seen that the actual burst signal fluctuates and is dominated by high frequency components. Moreover, it can be seen from Figure 8 that the residual signal does not have normal distribution. Hence the linear predictor does not provide the optimal prediction in the mean square error sense. Therefore, nonlinear models have to be considered to possibly obtain better models (see Section 5).

For the background signal $y(t)$, $5,000 \leq t \leq 7,500$, the SCAN and ESACF methods are also used to identify the orders of the tentative stationary or nonstationary models of the burst signal as ARMA($p + d, q$). Moreover, the augmented Dickey-Fuller Unit Root Test indicates that this signal should be considered as a nonstationary signal with unit root. Going to the first order incremental signal removes the unit root. Hence the tentative model transfer functions for the background signal are as follows:

$$\begin{aligned} \text{ARIMA}(3, 1, 2) : & \frac{(1 - 1.491L + 0.4955L^2)}{(1 - 1.823L + 0.8271L^2 + 0.02895L^3)} \\ \text{ARIMA}(2, 1, 3) : & \frac{(1 - 1.525L + 0.5532L^2 - 0.02452L^3)}{(1 - 1.854L + 0.8863L^2)} \\ \text{ARIMA}(5, 1, 1) : & \frac{(1 - 0.9903L)}{(1 - 1.309L + 0.1711L^2 + 0.04169L^3 + 0.09065L^4 + 0.07108L^5)} \\ \text{ARIMA}(4, 1, 2) : & \frac{(1 - 1.309L + 0.316L^2)}{(1 - 1.63L + 0.5931L^2 - 0.01815L^3 + 0.09992L^4)} \\ \text{ARIMA}(3, 1, 3) : & \frac{(1 - 0.7363L - 0.6627L^2 + 0.4075L^3)}{(1 - 1.085L - 0.5478L^2 + 0.6887L^3)} \\ \text{ARIMA}(0, 1, 5) : & \frac{(1 + 0.3859L + 0.3004L^2 + 0.28L^3 + 0.2142L^4 + 0.1295L^5)}{1} \end{aligned}$$

From the tentative models for the background signal, it turns out that ARIMA(5, 1, 1) is the best model for $y(t)$ in the sense that it has the smallest mean square error. Table 2 shows the mean square error for the one-step prediction of the background signal.

Although the diagnostic checking shown in Figure 10 reveals that the residual process of the background signal is not a white noise and does not have normal distribution, it is seen from Figure 9 that the one step prediction of the

Table 2: Mean square error for the prediction of the background signal from time point 5,000 to time point 7,500.

Model	Mean Square Error
ARIMA(3, 1, 2)	28, 014
ARIMA(2, 1, 3)	28, 007
ARIMA(5, 1, 1)	27, 636
ARIMA(4, 1, 2)	27, 658
ARIMA(3, 1, 3)	28, 149
ARIMA(0, 1, 5)	30, 348

Table 3: Mean square error for the ARIMA prediction from time point 7,501 to time point 160,000.

Model	Mean Square Error
Burst Model	87, 448
Background Model	44, 573
Switching Model	37, 078

background signal shows a reasonably good fitting with the actual background signal (small mean square error). Therefore, we decided to use this model to be the model for the background signal.

Although the log transformation is often used to convert time series that are nonstationary with respect to the innovation variance into stationary time series, the log transformation is not significantly improving the models for the burst and background signals.

4 Presence of Heteroskedasticity

Heteroskedasticity is the phenomenon that the residual error $\epsilon(t)$ of the model has time-varying conditional variance, that is, $E(\epsilon^2(t)|t-1)$ depends on the time t . Recall that under the condition that the best model has been obtained, the residual error $\epsilon(t)$ should be uncorrelated. However, $\epsilon^2(t)$ could be a correlated sequence and the heteroskedasticity test precisely checks whether the observed squared residual sequence is correlated enough, in which case the sequence is said to have ARCH (Auto Regressive Conditional Heteroskedasticity) effect.

For burst mode, the hypothesis of correlation of the residual error is rejected ($H(\epsilon(t) \text{ correlated}) = 0$) and the hypothesis of correlation of the residual squared sequence is accepted ($H(\epsilon^2(t) \text{ correlated}) = 1$). Hence the burst part has ARCH. For the background mode, both hypotheses of correlation of the sequence and the squared sequence are accepted. While we might be tempted to assert existence of ARCH effect in the background mode, it should be pointed out that the primary condition of lack of correlation of the residual sequence $\epsilon(t)$ does not hold, so that the observed correlation of $\epsilon^2(t)$ might in fact be coming from the correlation of $\epsilon(t)$. As such the ARCH effect in the background signal has not been positively established.

5 Nonlinear ACE Modeling

The residues of the ARIMA models for the burst and background signals do not have normal distribution. Hence the optimal predictors are not the linear predictors. This provides the clue that nonlinear models should be considered as possible candidates for the optimal predictors. However, the actual signal does not indicate what the nonlinear candidate models could be. The Alternating Conditional Expectation (ACE) is an appropriate modeling technique in the sense that the ACE method is nonparametric and the ACE algorithm converges to the optimal predictor [4]. The canonical correlation technique is used to estimate the order of the ACE models. For example, the first three canonical correlation coefficients of the incremental burst signal are found to be

$$\sigma_1 = 0.6891, \quad \sigma_2 = 0.3003, \quad \sigma_3 = 0.1389, \quad \dots$$

and the coefficients decay rapidly thereafter. Hence it is reasonable to keep only the first two coefficients, from which it transpires that the order of the incremental burst process is 2. Therefore, the ACE model of the burst signal appears to be

$$x(t) = \phi(x(t-1), x(t-2))$$

with a similar conclusion holding for the background signal. The mean square errors for the burst and background one step ACE predictors are 29,997 and 5,349.8, respectively, on the training set of the ACE models. These results compare well with those of ARIMA. The problem is that the ability of the ACE model to predict the signal outside the training set rapidly deteriorates, as shown in Table 4.

6 Switching Dynamics

From the mathematical models of the burst signal and background signal, the whole signal can be modeled as the signal obtained from switching between the burst model and the background model. The criterion to select which model has to be used at a particular time t is based on the absolute summation of the sample autocorrelations computed from the incremental signal $\{x(t-1), \dots, x(t-500)\}$. If the absolute summation of the sample autocorrelation is smaller than the threshold, we select the burst model. On the other hand, if the absolute summation of the sample autocorrelations is larger than the threshold, we select the background model. Comparison between the actual signal, the burst ARIMA prediction, the background ARIMA prediction, and the switching ARIMA prediction are shown in Figures 11 and 12. The mean square error for these prediction models computed from time point 7,501 to time point 160,000 are shown in Table 3.

Comparison between the actual signal, the burst ACE prediction, the background ACE prediction, and the switching ACE prediction are shown in Figures 13 and 14. The mean square errors for these prediction models computed from

Table 4: Mean square error for the ACE prediction from time point 7,501 to time point 160,000.

Model	Mean Square Error
Burst Model	86,120
Background Model	45,107
Switching Model	64,993

time point 7,501 to time point 160,000 are shown in Table 4. These results show that the switching ARIMA model provides better prediction for the actual signal than the switching ACE model. The reason for this is that ACE appears to be very sensitive to the training data it was constructed from, whereas ARIMA does not appear to suffer that defect.

7 Conclusion

The main conclusion is that the sEMG signal of NSA reveals a new class of complex nonlinear dynamic behavior in the sense that the difference between bursting and background signals is a matter of difference in dynamical behavior, much more than just a difference of amplitude or variance of the signal.

Switching among rhythms, e.g., gamma/delta, has recently received considerable attention from neurodynamicists [7, 6]. Simple 4 neurons models have indeed been able to reproduce this kind of behavior. However, a difference is that the gamma/delta transition is accompanied by a definite frequency shift, while, here, FFT analysis of the background to burst transition does not reveal a marked frequency shift, but the onset of an oscillation at a specific frequency higher than the peak of the background. The specificity of this switching is possibly related to the unique nature of the dural attachment feedback that generates it. On a slightly different tone, the ‘‘bursty’’ activity of the thalamus consisting of trains of spikes interrupted by periods of inactivity also bears some resemblance with the phenomena observed here.

Acknowledgements

This research was supported by the Association for Network Care (ANC).

References

- [1] *SAS/ETS User’s Guide, Version 8, 2 Vol. SET*. SAS Publishing, August 2000. ISBN: 1580254896.
- [2] A. Breig. *Adverse Mechanical Tension in the Central Nervous System*. John Wiley and Sons, New York, 1987.
- [3] A. Breig. *Skull Traction and Cervical Cord Injury: A New Approach to Improved Rehabilitation*. Springer Verlag, 1989. ISBN: 0387504141.
- [4] L. Breiman and J.H. Friedman. Estimating optimal transformations for multiple regression and correla-

tion. *Journal of the American Statistical Association (JASA)*, 80:580–598, 1985.

[5] J. D. Hamilton. *Time Series Analysis*. Princeton University Press, Princeton, New Jersey, 1994.

[6] C. Koch. *Biophysics of Computation: Information Processing in Single Neurons*. Oxford University Press, New York, New York, 1999. ISBN 0-19-510491-9.

[7] N. Kopell. We got rythm: Dynamical systems of the nervous system. *Notice of the AMS*, 47(1):6–16, January 2000.

[8] J. W. McDonald, D. Becker, C. Sadowsky, J. A. Jane, T. E. Conturo, and L. Schultz. Late recovery following spinal cord injury. *J. Neurosurg (Spine 2)*, 97:252–265, 2002.

[9] M. Panjabi. The stabilizing system of the spine. part i. function, dysfunction, adaptation, and enhancement. *Journal of Spinal Disorders*, 5(4):383–389, 1992.

[10] E. E. Selkurt. *Physiology*. Little, Brown and Company, Boston, 1971.

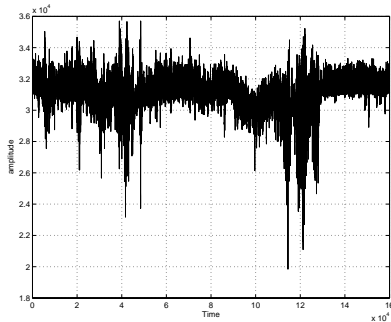


Figure 1: The full neck sEMG signal.

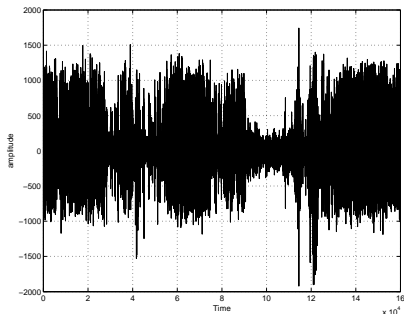


Figure 2: The incremental neck sEMG signal.

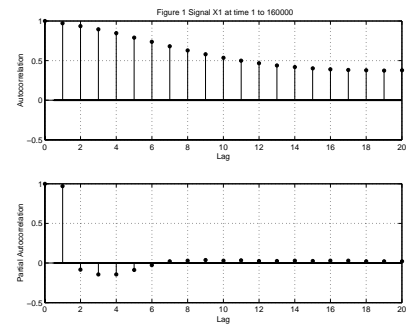


Figure 3: Autocorrelation and partial correlation of the full raw neck signal.

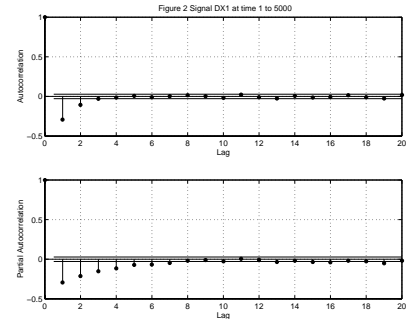


Figure 4: Autocorrelation and partial correlation of the incremental “burst” part of the neck signal.

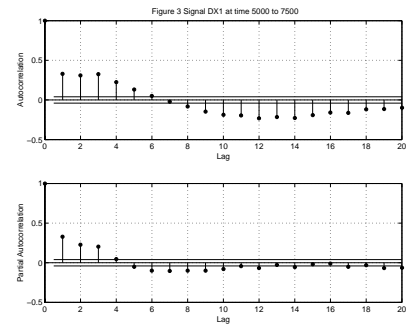


Figure 5: Autocorrelation and partial correlation of the incremental “background” part of the neck signal.

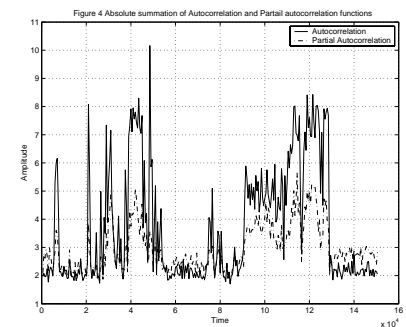


Figure 6: Plots of absolute summations of autocorrelation and partial correlation functions of the full neck signal versus T .

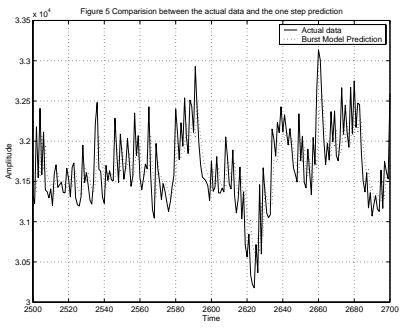


Figure 7: Fitting between the “burst” signal and the one step ARIMA predictor.

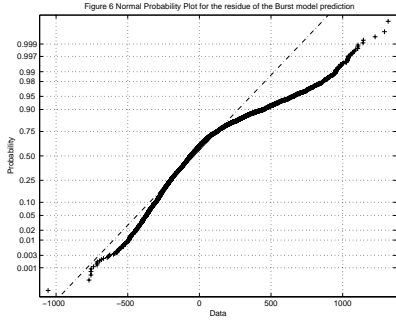


Figure 8: Test of Gaussian property of residual fitting error of “burst” signal.

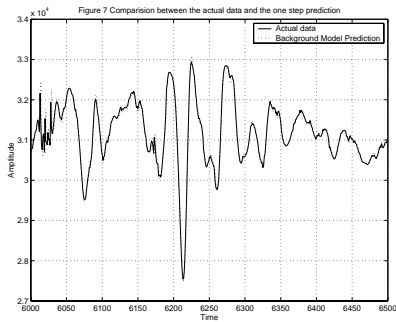


Figure 9: Fitting between the “background” signal and the one step ARIMA predictor.

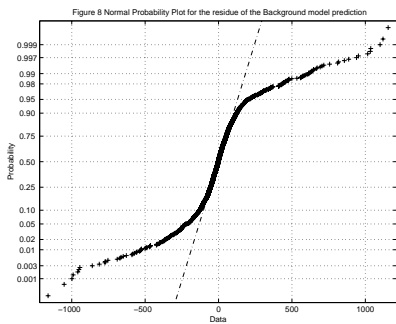


Figure 10: Test of Gaussian property of residual fitting error of “background” signal.

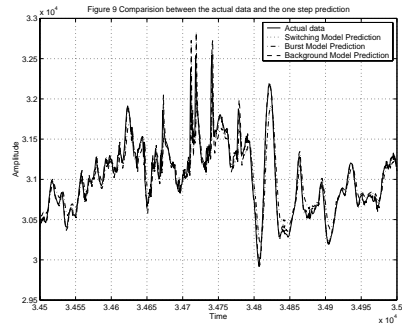


Figure 11: Comparison between actual (low frequency) signal and one step ARIMA predictors.

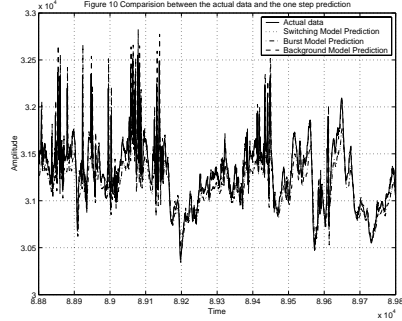


Figure 12: Comparison between actual (high frequency) signal and one step ARIMA predictors.

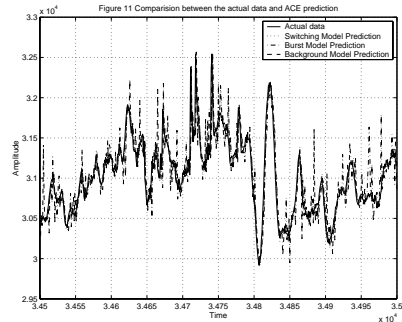


Figure 13: Comparison between actual (low frequency) signal and one step ACE predictors.

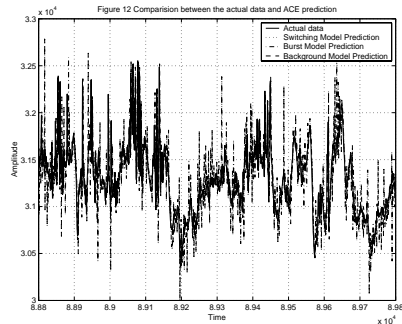


Figure 14: Comparison between actual (high frequency) signal and one step ACE predictors.